Chalcogenide Letters Vol. 6, No. 4, April 2009, p. 155 - 161

# EFFECT OF ANTIMONY INCORPORATION IN $CuInS_2$ THIN FILMS

M. Ben Rabeh*, N. Chaglabou, M. Kanzari
*Laboratoire de Photovoltaïque et Matériaux Semi-conducteurs -ENIT BP 37, Le belvédère 1002-Tunis, Tunisie*

Structural optical and electrical properties of undoped and Sb-doped $CuInS_2$ thin films grown by single source thermal evaporation method on corning 7059 glass substrates heated at 100°C were studied. Sb species was mixed in the starting powders. The amount of the Sb source was determined to be in the range 0-4 Wt % molecular weight compared with the $CuInS_2$ alloy source. The films were annealed in vacuum at temperature of 200°C for 2h. The effect of vacuum annealing on the properties of the films was studied by means of X-ray diffraction (XRD), optical reflection and transmission and resistance measurement. All the $CuInS_2$/Sb films have relatively high absorption coefficient between $2\times10^4 cm^{-1}$ and $10^5 cm^{-1}$ in the visible and the near-IR spectral range. We found that only $CuInS_2$ thin films with high Sb incorporation exhibit p-type conductivity.

(Received March 20, 2009; accepted April 6, 2009)

*Keywords*: Thin films; Chalcopyrite; $CuInS_2$; doping; Antimony.

## 1. Introduction

Ternary chalcopyrite $CuInS_2$ thin films exhibit many excellent physical and chemical properties such as high absorption coefficient of almost $10^5 cm^{-1}$ in the visible spectral range [1], high tolerance to the presence of defects [2], an direct band gap closes to 1.5 eV, the optimum value for the photovoltaic conversion of solar energy [3], possibility to avoid n and p-type conductivity [4] and high chemical stability. In contrast to other ternary semiconductor materials, $CuInS_2$ is nontoxic, low-cost and easy to fabricate by various thin film deposition techniques [5-7]. For controlling a conduction type and obtaining a low resistivity, several impurities doped $CuInS_2$ bulks have been studied. In several studies, it was shown that the structural, optical and electrical properties of $CuInS_2$ thin films could be obviously improved by optimized deposition conditions and doping [8-10]. Additionally, the electrical properties of $CuInS_2$ thin films could be modified by thermal in a reducing atmosphere [11,12].Akaki et al [13] studied the structural, electrical and optical properties of Bi-$CuInS_2$ thin films grown by vacuum evaporation method. Zribi et al [8] investigated the effect of Na doping on the properties of $CuInS_2$ thin films and obtained more interesting results. The incorporation of iron during the crystal growth of $CuInS_2$ by chemical vapor transport was studied [14.15] and the results of electrical and photoluminescence measurements of Phosphor-doped and Zn-doped $CuInS_2$ crystals were reported [16]. T. Yamamoto et al [9] investigated the electronic structures of n-type doped $CuInS_2$ crystals using Zn and Cd species and showed that p-type doping using the group V elements such as N, P and As increases the Madelung energy, which gives rise to instability of ionic charge distribution in p-type doped $CuInS_2$ crystals [17]. Enzenhofer et al [10] showed that the open circuit voltage of solar cells based on $CuInS_2$ can be enhanced via controlled doping of small amounts of Zinc. In our previous paper [18] the incorporation of the doping element Sn in $CuInS_2$ was succeeded by annealing the Sn-doped films in vacuum. In this paper, we report on structural, optical and electrical properties of the Sb-doped $CuInS_2$ thin films before and after annealing in vacuum.

* Corresponding author: mohamedbenrabeh@yahoo.fr

## 2. Experimental

### 2.1. Synthesis of targets and films

Amount of the elements of 99.999% purity Cu, In, S and Sb, five different powders of $CuInS_2$/Sb (0,1,2,3 and 4 wt % molecular weight) were prepared. X-rays diffraction of powders analysis showed that in all cases the principal phase present in the ingots is the $CuInS_2$. Crushed powder of every ingot was used as raw material for the thermal evaporation. The Sb-doped $CuInS_2$ thin films were deposited by single source thermal evaporation method on corning 7059 glass substrates heated at 100 °C with a base pressure at $10^{-6}$ torr. After what the films were annealed in vacuum at temperature of 200°C for 2 h.

### 2.2. Characterization techniques

The structures of the $CuInS_2$/Sb samples were investigated using D8 Advance diffractometer. The optical characteristics were determined at normal incidence in the wavelength range 300 to 1800 nm using a Shimadzu UV/Vis-spectrophotometer. The resistance was measured using a digital universal meter and the type of conductivity of these films was determined by the hot probe method. Film thicknesses were measured by interference fringes method **[19]** and were in the range of 450-750 nm.

## 3. Results and discussion

### 3.1. Structural properties

Fig. 1 shows the X-ray diffraction patterns of undoped and Sb-doped $CuInS_2$ thin films before annealing. It can be seen that samples presented a peak at $2\theta = 27.9°$ assigned to the (112) reflection of $CuInS_2$ phase for the samples doped 0, 1,2 and 3 % Sb molecular weight and become highly oriented when the Sb content is 4 % molecular weight. The intensity of the (112) reflection increases with increasing antimony content and it was found that Sb with 4% molecular weight enhanced the growth of $CuInS_2$ phase with good crystallinity. We note also some additional diffraction peaks at 26.49° and 43.4°, which can be associated to binary compounds $In_6S_7$ and Cu crystal. Figure 2 shows the X-ray diffraction patterns of the films after annealing in vacuum at temperature of 200°C for 2 h. All the annealed films are oriented (112) plane and there is an improvement in the growth of the films after annealing for all the samples containing antimony. We note also the persistence of minor peaks with lower intensities, associated to copper Cu and $In_6S_7$ phases.

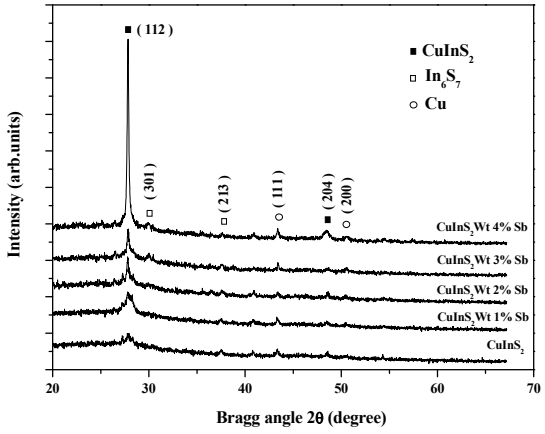


*Fig. 1. X-ray diffraction patterns of $CuInS_2$ thin films with different Sb % molecular weight.*

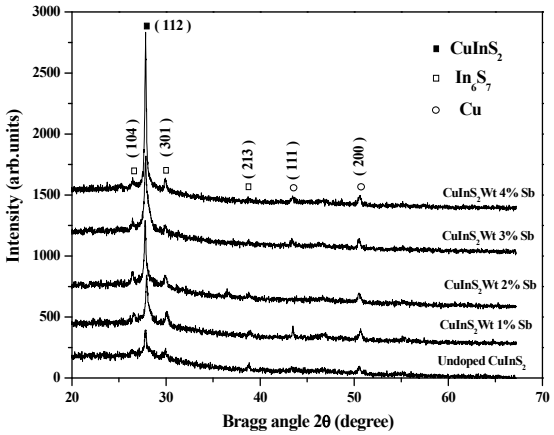


*Fig. 2. X-ray diffraction patterns of $CuInS_2$ thin films with different Sb % molecular weight after annealing in vacuum.*

In the other hand the grain size along the (112) peaks were evaluated using the Debye Scherer relation:

$$L = \frac{0.9\lambda}{\cos\theta_0 \Delta(2\theta)} \tag{1}$$

Where λ is the wavelength of the X-ray radiation used, Δ(2θ) the half intensity width of the peak and $\theta_0$ the Bragg angle. Fig. 3 shows the behaviour of grain size versus the Sb % molecular weight before and after annealing. As we can see from figure 3 the grain size are in the range 10-51nm before annealing and in range 33-53nm after vacuum annealing. We found that the grain size increases with increasing Sb % molecular weight. The maximum value was obtained for 4 Sb % molecular weight before and after vacuum annealing. This result confirmed the XRD analysis and optical properties which shows an improvement of the crystallinity at this % Sb molecular weight with low transmission values.

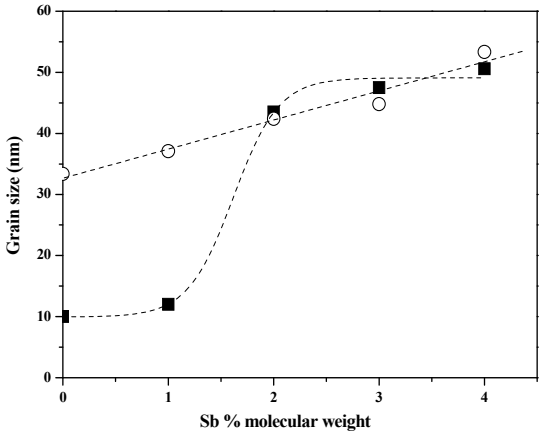


*Fig. 3. Variation of the grain size of $CuInS_2$ thin films with different Sb % molecular weight (Square) before annealing and (Circle) after annealing.*

### 3.2. Optical properties

Figures 4 and 5 shows optical transmission spectra in the wavelength range 300-1800nm at normal incidence for undoped and Sb-doped $CuInS_2$ with different Sb content before and after vacuum annealing. We note a decrease in the transmission values with increasing Sb % molecular weight before and after vacuum annealing. Probably, antimony atoms are localized in the volume rather near the surface. We note also an improvement in sharp fall of the transmission at the band edge after annealing which is an indication of good crystallinity.

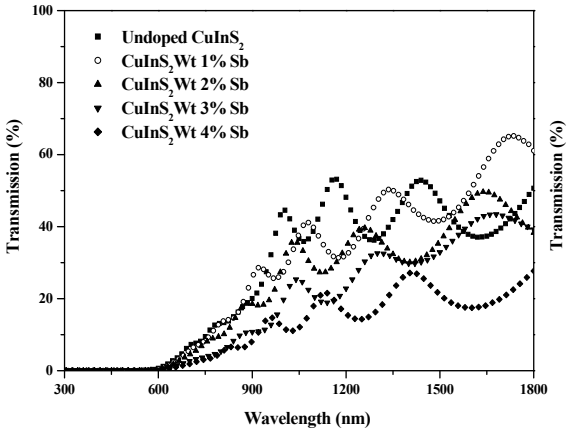


*Fig. 4. Optical transmission of $CuInS_2$ thin films with different Sb % molecular weight.*

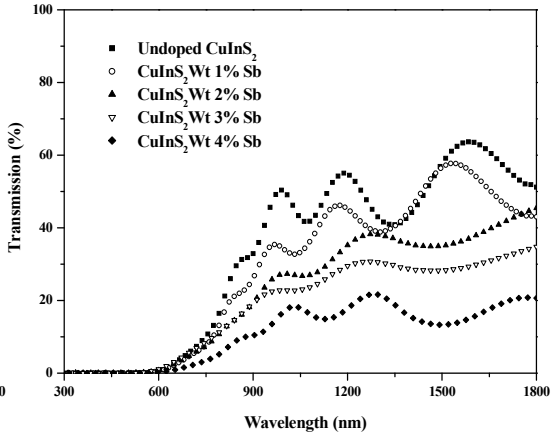


*Fig. 5. Optical transmission of $CuInS_2$ thin films with different Sb % molecular weight after annealing in vacuum.*

To calculate the absorption coefficient *α(hv)*, the following relation was used [20].

$$\alpha = \frac{1}{d}\ln\left[\frac{(1-R)^2}{T}\right] \tag{2}$$

Where *d* is the film thickness, R and T are the reflection and transmission coefficient, respectively. Figure 6 shows the dependence of the absorption coefficient α versus the photon energy *hv* of the Sb-doped $CuInS_2$ thin films before annealing. The films have relatively high absorption coefficients in the range 2 $10^4$cm$^{-1}$ to 4 $10^4$cm$^{-1}$ in the visible. The absorption coefficient increases with increasing Sb % molecular weight. Figure 7 shows the absorption coefficients versus the photon energy for the Sb-doped $CuInS_2$ thin films after annealing in vacuum. All the films have relatively high absorption coefficients more than $2.10^4$ cm$^{-1}$ and the higher values are obtained for the $CuInS_2$ samples doped 4 Wt % Sb molecular weight.

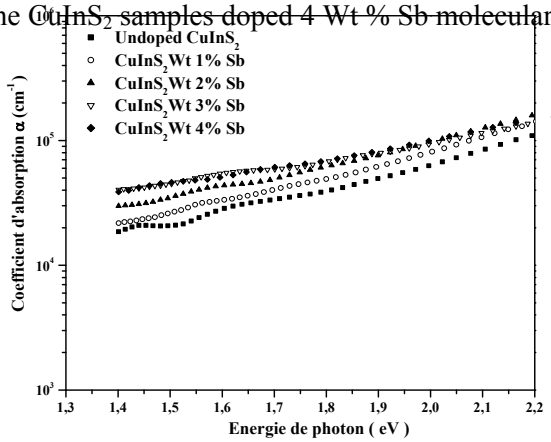


*Fig. 6. Absorption coefficients spectra of $CuInS_2$ thin films with different Sb % molecular weight.*

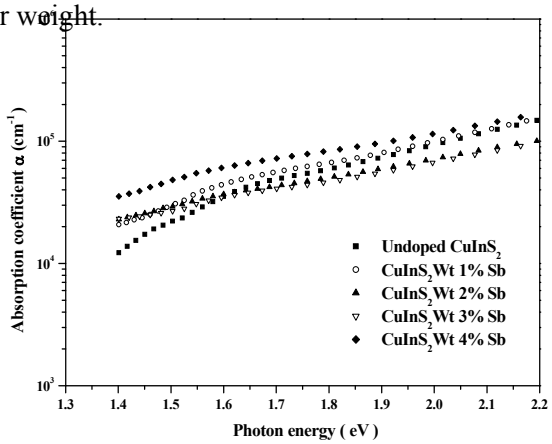


*Fig. 7. Absorption coefficients spectra of $CuInS_2$ thin films with different Sb % molecular weight after annealing in vacuum.*

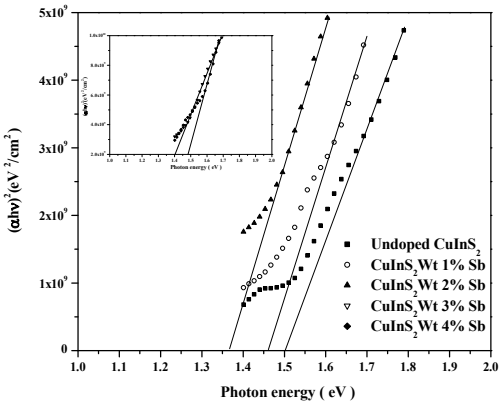


*Fig. 8. Relationship between $(\alpha hv)^2$ and photon energy of Sb-doped $CuInS_2$ thin films with different Sb % molecular weight.*

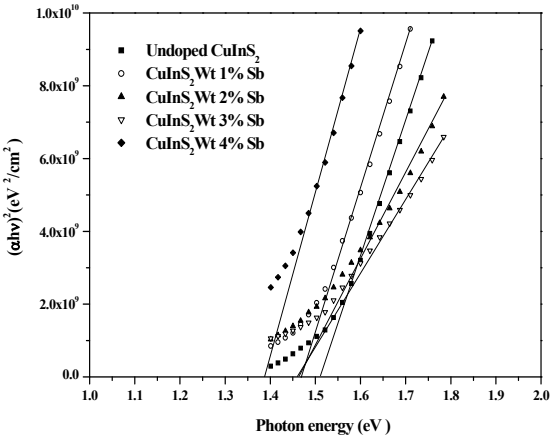


*Fig. 9. Relationship between $(\alpha hv)^2$ and photon energy of Sb-doped $CuInS_2$ thin films with different Sb % molecular weight after annealing in vacuum.*

The relation between the absorption coefficients α and the incident photon energy ($hv$) can be written for direct allowed band gap as:

$$(\alpha h\nu)^2 = A(h\nu - Eg) \tag{3}$$

Where 'A' is constant and $E_g$ is the optical band gap. To determine optical transition, $(\alpha hv)^2$ versus $hv$ was plotted, and the corresponding band gaps were obtained from extrapolating the straight portion of the graph on the $hv$ axis at $(\alpha hv)^2 = 0$ (Figures 8 and 9). It is now well established that $CuInS_2$ is a direct gap semiconductor [21], with the band extrema located at the centre of the Brillouin.

The direct band gap (Table 1) energy are in the range 1.37-1.50 eV for samples before annealing and in the range 1.38–1.51eV for samples annealed in vacuum.

*Table 1. Values of the optical band gap energy of Sb-doped $CuInS_2$ as function of Sb% molecular weight before and after vacuum annealing.*

| | $E_g$ (eV) | |
|---|---|---|
| CIS/Sb | Before annealing | After annealing |
| Undoped | 1.502 | 1.510 |
| Sb 1% | 1.461 | 1.470 |
| Sb 2% | 1.370 | 1.465 |
| Sb 3% | 1.404 | 1.460 |
| Sb 4% | 1.485 | 1.382 |

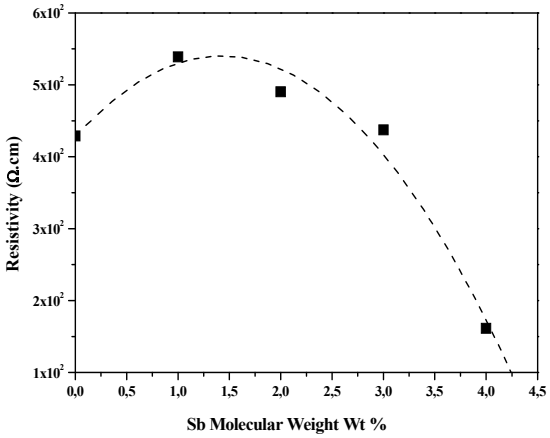


*Fig. 10. Resistivity versus Sb % molecular weight of Sb-doped $CuInS_2$ thin films after annealing in vacuum.*

### 3.3. Electrical properties

Besides the optical properties, the electrical properties are also an important aspect of the performance of Sb-doped $CuInS_2$ thin films. Before annealing, as-deposited and Sb-doped $CuInS_2$ samples are highly compensated and no significantly conduction type is observed. One of the reasons is that the concentration of donor and/or acceptor impurities in all $CuInS_2$ samples may not change by Sb doping .After annealing in vacuum (figure 10), all the films presented moderate higher electrical resistivity with low P-type conductivity for the samples doped wt 4% Sb molecular weight. The resistivity increases from $4.3x10^2$ Ω cm (0% Sb) to $5.3x10^2$ Ω cm (1.5 % Sb) after what it decreases by increasing Sb % molecular weight until $5.3x10^2$ Ω cm. The samples doped with 4 % Sb molecular weight show the minimum of resistivity with p type conductivity. So how we can explain the p-conductivity in our case for the high Sb incorporation? Since there are so many intrinsic defects such as In interstitial ($In_i$) and/or S vacancy ($V_s$). We consider that the introduced Sb acceptor with low amount (< 4% molecular weight) cannot compensate the donors sufficiently. It was also found [22] that p-type $CuInS_2$ crystals could be obtained by Sb-doping. It was suggested that the Sb atoms in the S site might enhance p-type conductivity [22]. Consequently it is probable that antimony in our case occupies the sulfur site to make an acceptor which can explain the origin of the p-type conductivity.

## 4. Conclusions

The effects of antimony incorporation on the structural, optical and electrical properties of $CuInS_2$ thin films were studied. Sb species was mixed in the starting powders for different Sb % molecular weight. undoped and Sb doped $CuInS_2$ thin films grown by single source thermal evaporation method on corning 7059 glass substrates heated at 100°C were deposited and subsequently annealed in vacuum at temperature of 200°C for 2h. The absorption coefficients deduced from optical measurements are greater than $2.10^4 cm^{-1}$ in the range 1.4-2.2 eV and become constant along the visible spectral range with a value of $10^5$ $cm^{-1}$ for the $CuInS_2$ doped wt 4% Sb molecular weight after vacuum annealing. The Sb-doped samples after annealing have bandgap energy of 1.38-1.51 eV. Only $CuInS_2$ samples doped with high percent of Sb incorporation (4% Sb molecular weight) exhibit p-type conductivity.

## References


[1] K. Siemer, J. Klaer, I. Luck, J. Bruns, R. Klenk, D. Braunig, Sol. Energy Mater. Sol. Cells **67**, 159-166 (2001).

[2] Aksenov I and Sato K 1992 Japan. J. Appl. Phys. 31 2352.

[3] R. Scheer, K. Diesner, H.-J. Lewerenz, *Thin Solid Films* **168**, 130 (1995).

[4] J. L. Shay and J. H. Wernick. Ternary Chalcopyrite Semiconductors, Growth, Electronic Properties and Applications ( Pergamon Press, New York, 1975).

[5] T. Hashimoto, S. Merdes, N. takayama, H. Nakayama, H. Nakanishi, S.F. Chichibou, S. Ando, in: W. Palz, H. Ossenbrink, P. Helm (Eds.), 20th European Photovoltaic Solar Energy Conference, Proceedings of the International Conference, Barcelona, June 6 – 10, 2005 p. 1926.

[6] M. Zribi, M. Kanzari, B. Rezig, in: W. Palz, H. Ossenbrink, P. Helm (Eds.), 20th European Phtovoltaic Solar Energy Conference, Proceedings of the Internatinal Conference, Barcelona, June 6– 10, 2005, p. 1890.

[7] J. S. NcNatt, J.E. Dickman, A.F. Hepp, C.V.Kelly, M.H.C. Jin, K.K. Banger, Conference Record of the 31st IEEE Photovoltaic Specialists Conference, Lake Buena vista, Florida, january 3 – 7, 2005, p. 375.

[8] M. Zribi, M. Kanzari, B. Rezig, Jpn J. Appl. Phys. **29**, 203- 207 (2005).

[9] Tetsuya Yamamoto, Ilka V. Luck, Roland Scheer, Applied Surface Science **159** – **160**, 350-354 (2000).

[10] Tobias Enzenhofer, Thomas Unold, Roland Scheer, Hans-Werner Schock, Material Research Society, 2005 Spring Proceedings, San Francisco, CA Spring Meeting March 28-April 1 2005.

[11] M. Abaab, M. Kanzari, B. Rezig, M. Brunel, Solar Energy Materials & Solar Cells **59**, 299-307 (1999).

[12] M. Ben Rabeh, M. Kanzari, B. Rezig, Thin Solid Films **515,** 5943 - 5948 (2007).

[13] Y.Akaki, H. Matsuo and K. Yoshino, *Phys Stat Sol (c)* **8**, 2597 (2006).

[14] G. Brandt, A Ranber, J Schneider, Solid St.Commun. **12**, 481 (1983).

[15] J.J.M. Binsma, L.J Giling, J.Bloem, J. Lumirrex. **27**, 35 (1982).

[16] H.Y. Uengt, H.L. Hwang, J. Phys. Chem. Solids. **51**, 11 (1990).

[17] T. Yamamoto, H.K. Yoshida, Jpn. J. Appl. Phys. **35**, L1562 (1996).

[18] M. Ben Rabeh, M. Zribi, M. Kanzari, B. Rezig, Materails Letters **59**, 3164–3168 (2005).

[19] O.S. Heavens, Optical Properties of thin Solid Films, Butterworths, London, 1950.

[20] D.E. Milovzorov, A.M. Ali, T. Inokuma, Y. Kurata, T. Suzuki, S. Hasegawa, Thin Solid Films **382**, 47 (2001).

[21] N.N.Nishikawa, I. Aksenov, T.Sinzato, T.Sakamoto and K.Sato, Japan.J.Appl.Phys; **34**, L975 (1995).

[22] Y. Akaki, H. Komaki, H. Yokoyama, K. Yoshino, K. Maeda, T. Ikari, Journal of Physics and Chemistry of Solids; **64**, 1863 (2003).